

Measurement of Alcohol Thermal Conductivities Using a Relative Strain-Compensated Hot-Wire Method

J. David Raal* and Robert L. Rijdsdijk

Chemical Engineering Research Group, Council for Scientific and Industrial Research, Pretoria 0001, South Africa

Thermal conductivities and temperature coefficients are presented for 10 alcohols from methanol to decanol for the temperature range -20 to 80 °C. Measurements were made with a two-wire cell designed to eliminate strain, thermocouple, and end effects. Twin cells were used in a relative configuration with a constant energy dissipation in each. The reference liquid in one of the cells was ethylene glycol, selected for its appreciable viscosity and availability of data. For the case of a varying energy dissipation rate a correction factor, obtained from an iterative numerical solution of Fourier's equation, is given. The smooth periodic variation of temperature coefficient with number of carbon atoms for the alcohol series, not previously found, merits further study.

Introduction

Accurate measurement of fluid thermal conductivity as a function of temperature and pressure has long presented a considerable challenge to experimenters, as a survey of disparities in available data will readily attest.

Steady-state methods, which typically involve measurement of a uniform thermal flux between isothermal surfaces such as concentric cylinders, are time consuming and subject to errors due to surface and end effects and to free convection which is not readily detected in this type of equipment. Failure to account for radiative energy transport in liquids with small infrared absorption can produce an apparent dependence on the thickness of the liquid layer (1).

Measurements by steady-state methods still account for a large portion of the available literature data which are often unreliable. Steady-state methods are being superseded by transient hot-wire methods.

The transient hot-wire method involves measurement of the temperature rise of an electrically heated wire, immersed in the fluid, over a comparatively short time and is applicable to electrically nonconducting liquids and gases.

The method, due originally to Stålhane and Pyk (2), has been developed and refined by many investigators (3-12). The difficulties experienced by earlier workers (3-5) in designing equipment that could closely approximate a line source in an infinite fluid, for which the theory has now been well developed, have been largely overcome by the use of very fine heating wires and two-wire cells, and by advances in electronics.

Among numerous potential sources of error the more important appear to be those due to free convection in the fluid, conduction end effects which perturb the temperature field from the ideal radial one, temperature reflection at the boundary walls, finite wire thermal capacity, a nonconstant heating rate, and spurious thermocouple and strain effects.

Excellent results were obtained by De Groot, Kestin, and Sookiazian (11) in the measurement of thermal conductivities of noble gases at pressures up to 34.5 mPa. Their thermal conductivity cell, adapted from the design proposed by Haarman (13), incorporates two 5- μ m platinum wire elements of different

lengths contained in two arms of an automatic Wheatstone bridge. This bridge is sensitive to the resistance difference of the wires, and the arrangement functions effectively as if a portion of a line source were active.

Experimental conditions were chosen (11) to keep the heating rate effectively constant, to eliminate influences from the containing boundaries, and to reduce the temperature jump at the wire surface. Unlike earlier measurements, the values of the Eucken factor $\lambda/[\eta C_V F(T)]$ for the four monatomic gases studied were remarkably close to the value (2.50) demanded by the Chapman-Enskog solution of the Boltzmann equation (14), and it was concluded that the instrument functioned exactly like a line source in an infinite fluid. Measurements were made only at room temperature.

Similar equipment was used by De Castro and Wakeham (15) to measure the thermal conductivity of *n*-heptane over a very small temperature range. The remarkable sensitivity to vertical alignment reported (15) was most likely due to a design weakness in the equipment as this sensitivity was not found by Gillam and Lamm (6) or by us.

An attractive variation of the absolute transient method is the relative transient method proposed by Grassmann and co-workers (16-18), in which twin hot-wire cells are used. The wires are elements of two identical Wheatstone bridges, and the resulting diagonal voltages are led to the axes of an x-y recorder. From the slope of the linear portion of the resulting plot, the thermal conductivity of the test fluid is obtained relative to that of the reference fluid. Absolute values of energy dissipation and wire length are not required.

The method is very rapid once an equipment constant has been determined as a function of temperature. The departure from linearity of the plot gives an immediate indication of operating or equipment error. Also, factors which may cause some departure from the theoretical relationship between temperature rise and the logarithm of time, and which must be allowed for in absolute methods, tend to have a lesser influence when measuring a ratio of two cell responses. The onset of free convection is immediately detected and so eliminated.

As part of a program to develop experimental facilities for very accurate measurement of certain thermodynamic and transport properties of coal-derived liquids, we have developed a procedure combining elements of the two-wire cell of De Groot et al. (11) and the two-cell relative method of Grassmann and co-workers (16-18).

The equipment and the procedure are given in detail since we feel that further presentations of new data without careful analysis of equipment performance and error would be of limited use. Thermal conductivity data are presented for aliphatic alcohols from methanol to 1-decanol. Measurement capability will be extended to 400 °C and 50 mPa with a high-pressure modification of the cell described below.

Theory

Heat Transfer from a Line Source. Heat transfer from a line source is governed by the Fourier equation:

$$\frac{\partial T}{\partial t} = K \left[\frac{\partial^2 T}{\partial r^2} + \frac{1}{r} \frac{\partial T}{\partial r} \right] \quad (1)$$

* Address correspondence to this author at the Department of Chemical Engineering, University of Natal, Durban 4001, Republic of South Africa.

where $K = \text{thermal diffusivity} = \lambda/C\rho$. Appropriate boundary conditions are

$$\Delta T(r,t) = 0 \quad t \leq 0 \quad (2a)$$

$$\Delta T(r,t) = 0 \quad t \geq 0, r = \infty \quad (2b)$$

$$\lim_{r \rightarrow 0} (r \partial T / \partial r) = -q(2\pi\lambda) \quad t \geq 0, r = 0 \quad (2c)$$

The solution for a constant heating rate per unit source length q is well-known (19) and can be presented in the form

$$\Delta T(r,t) = [q/(4\pi\lambda)] Ei(4Kt/r^2) \quad (3)$$

For small values of $\zeta = r^2/(4Kt)$ the exponential integral is satisfactorily described by

$$Ei(\zeta) = \int_{\zeta}^{\infty} (e^{-\nu}/\nu) d\nu = -\gamma - \ln \zeta + \zeta - \zeta^2 \quad (4)$$

where $\gamma = \text{Euler's constant} = 0.5772$. Thus, after a certain period of time

$$\Delta T(r,t) = [q/(4\pi\lambda)] [-0.5772 + \ln(4Kt/r^2)] \quad (5)$$

In practice, the line source is replaced by a metal wire of radius a and finite thermal capacity per unit volume $\rho_w C_w$ and thermal conductivity λ_w . Solution of two coupled Fourier equations in this case (19, 20) (for the regions $0 < r < a$ and $a < r < \infty$) indicates that a correction factor

$$F = [1 - a^2(\rho_w C_w - \rho C)/(2\lambda t)] \quad (6)$$

must be introduced as a multiplier for the last term in eq 5 (the density and the heat capacity without subscripts in eq 6 refer to fluid properties).

The correction term in eq 6 is small for thin wires (5–20 μm) but is readily calculated and should be examined at time values of interest since it occurs as a multiplying factor in the slope of the ΔT vs. $\ln t$ plot used in absolute methods. For a platinum wire of 0.02-mm diameter, as used in the present study, F exceeded 0.997 for $t \geq 1$ s.

Errors arising from the fluid-containing walls, where temperature reflection may occur after a sufficiently long time, have been studied by several investigators (8, 10, 20). This error source is easily eliminated by proper cell design. For large values of cell to wire diameter (e.g., $b/a > 2000$), the onset of free convection will for most systems precede reflection at the boundaries, and the latter need not be considered. Radiation errors are generally negligible (8) particularly at moderate temperatures.

For measurements in gases the rapid onset of convection restricts the time available for measurement, and initial effects must be reduced by using wires of low thermal capacity, i.e., thin wires. Temperature jump at the wire surface must then be considered, and to obtain the proper reference temperature, to which the measured thermal conductivity corresponds, a correction is added to the nominal fluid temperature (20).

Constancy of Heating Rate. The many solutions of eq 1 presented in the literature for boundary conditions describing or approximating a line source are usually obtained for a constant heating rate. In practice the heating rate will increase during the measurement unless circuit components for heating and temperature or resistance monitoring are carefully chosen. The problem has been examined briefly by De Groot et al. (19) and by Gillam and Lamm (8).

If heat is liberated in a line source at a nonconstant rate $q(t)$, the temperature distribution is given (19) by

$$T(r,t) = \frac{1}{4\pi\lambda} \int_0^t q(t') e^{-r^2/[4K(t-t')]} \frac{dt'}{t-t'} \quad (7)$$

Let $\tau' = 4Kt'/r^2$ and $\tau = 4Kt/r^2$

$$\therefore 4\pi\lambda T(r,t) = \int_0^{\tau} q(\tau') e^{-1/(\tau-\tau')} \frac{d\tau'}{\tau-\tau'} \quad (7a)$$

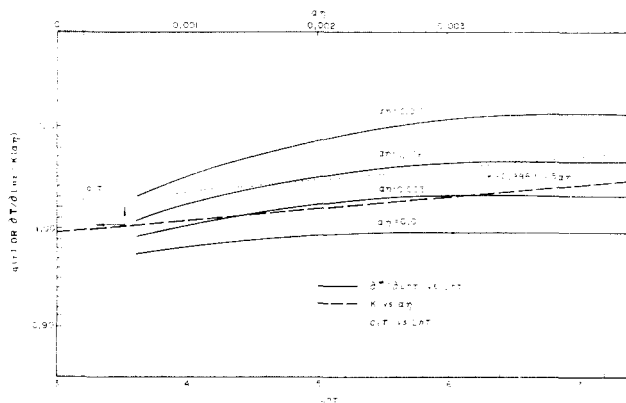


Figure 1. Correction factor for nonconstant heating rate.

The heating rate $q(t) = -2\pi r \lambda \partial T / \partial r|_{r=0}$ is not known a priori, but, for experiments in which a heated wire forms part of a Wheatstone or similar bridge, it is readily shown (8) that to a close approximation

$$q(t) = q_0 [1 + \alpha \eta \bar{T}(t)] \quad (8)$$

η is a function only of bridge resistances (see below), and α is the temperature coefficient of resistance of the heated wire material defined by $R' = R^0(1 + \alpha \Delta T)$. Substituting eq 8 into eq 7a gives

$$\bar{T} = \frac{4\pi\lambda}{q_0} T(r,t) = \int_0^{\tau} [1 + \alpha \eta \bar{T}(\tau')] e^{-1/(\tau-\tau')} \frac{d\tau'}{\tau-\tau'} \quad (9)$$

Equation 9 was integrated for a range of dimensionless time (τ) and $\alpha \eta$ values by a rapidly converging iterative procedure utilizing eq 5 as an initial estimate for $\bar{T}(\tau')$. Values of $\bar{T}(\tau')$ at intermediate values of τ' , required in the integration, were generated by using polynomial interpolation as given by Shampine and Allen (21). The results of the computations, using Romberg integration according to a program by Davis and Rabinowitz (22), are shown in Figure 1 and can be summarized as a correction to eq 5 in the form

$$\partial \bar{T} / \partial \ln \tau = K(\alpha \eta) = 0.996 + 11.5(\alpha \eta) \quad (10)$$

Figure 1 indicates that for $\alpha \eta < 0.006$ a linear relationship still exists between temperature and the logarithm of time for $\ln \tau > 6.0$ if heating rates are in accordance with eq 8. The slope of a ΔT vs. $\ln t$ plot, as used in absolute methods would, however, yield an incorrect thermal conductivity.

For cells using either a single heated wire or two heated wires and a bridge arrangement as shown in Figure 2, A and B, the heating rate for small ΔT is closely approximated by (6, 11)

$$q(t) = q_0 [1 + \alpha \eta \Delta T]$$

with

$$\begin{aligned} \eta &= (R_2 - R_1^0)/(R_2 + R_1^0) \quad (\text{single wire}) \\ &= [R^0 - 2(R_1^0 + R_2^0)]/R^0 \quad (\text{two wires}) \end{aligned}$$

where $R^0 = R_1^0 + R_2^0 + R_1' + R_2'$ (subscript 0 denotes value at start of heating period).

It is evidently much simpler to operate the bridge so that $\eta = 0$ (i.e., $R_1^0 = R_2$ (single-wire cell), $R_1' + R_2' = R_1^0 + R_2^0$ (two-wire cell)) than to correct for a nonconstant heating rate. Where this precaution has been neglected, however, it is recommended that the slope of a temperature vs. \ln (time) plot be corrected according to eq 10. For platinum, $\alpha = 0.0035$ so that a maximum correction in the thermal conductivity of $\sim 3\%$ would be required in the least favorable circumstances.

Equipment Response and Cell Constant. The apparent resistance change in an electrically heated wire may be a

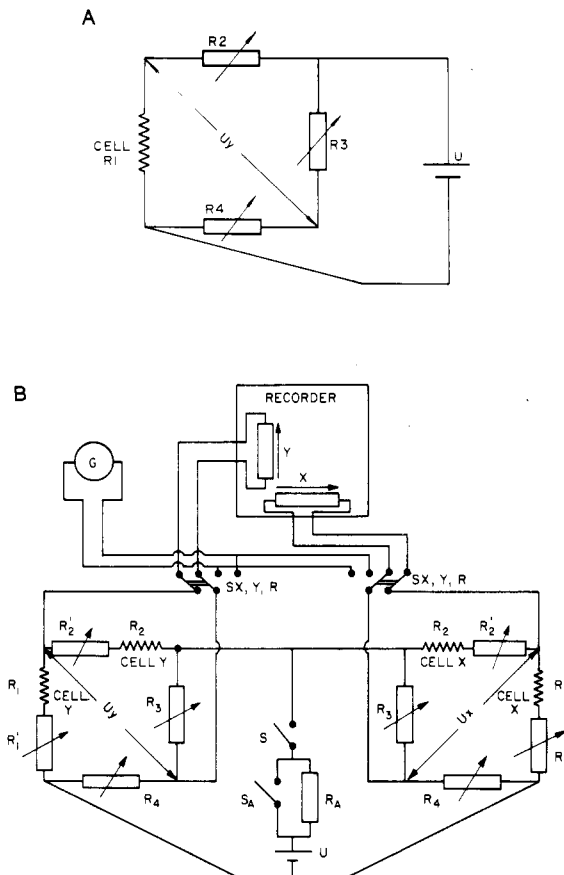


Figure 2. (A) Bridge arrangement for cell with single heated wire. (B) Schematic diagram of twin Wheatstone bridge arrangement.

function of thermocouple, strain, and end effects. If these spurious effects are assumed to be proportional to the temperature rise ΔT , the resistances of two heated wires in a thermal conductivity cell at time t are given by

$$R_1^t = R_1^0(1 + \alpha\Delta T) + k_1\Delta T \quad (11a)$$

$$R_2^t = R_2^0(1 + \alpha\Delta T) + k_2\Delta T \quad (11b)$$

For the arrangement shown in Figure 2B the diagonal bridge voltage U_y is related to the temperature rise and the bridge resistances by

$$\frac{U_y}{U} = \frac{\alpha\Delta T(R_1^0 R_2'^0 - R_2^0 R_1'^0) + \Delta T(k_1 - zk_2)(R_2^0 + R_2'^0)}{R^0 R^t} \quad (12)$$

R = total resistance in one arm of the bridge = $R_1 + R_1' + R_2 + R_2'$ and $z = (R_1^0 + R_1'^0)/(R_2^0 + R_2'^0)$.

Equation 12 (derived in the Appendix) confirms that the equipment response, U_y , is sensitive to the resistance difference $R_1^0 R_2'^0 - R_2^0 R_1'^0$, a feature which aids the elimination of end effects due to axial conduction at the wire terminals. If thermocouple and/or strain effects arising from the short and long heated wires in a cell (represented by the coefficients k_1 and k_2) are to be eliminated, eq 12 suggests that the resistances R_1' and R_2' be adjusted according to

$$R_1^0 + R_1' = R_2^0 + R_2' \quad (13)$$

i.e., $z = 1$, assuming $k_1 = k_2 = \text{constant}$.

In practice we have found it more advantageous to ensure a constant heating rate ($\eta = 0$, i.e., $R_1' + R_2' = R_1^0 + R_2^0$) than to satisfy eq 13. A useful feature of the two-wire bridge arrangement is that the resistance difference

$$A = R_1^0 R_2'^0 - R_2^0 R_1'^0 \quad (14)$$

can be chosen to be large (to magnify the equipment response) or zero to test for extraneous influences represented by the last term in eq 12. It may be noted here that in a test of the equipment, described below, operation with $A = 0$ produced a barely detectable response ($U_y < 1$ mV) at room temperature. At higher or lower temperatures a small residual response was detected, but this is allowed for in the cell constant required by the relative (two-cell) method.

The principal measurement in the twin bridge relative method used in the present study is the slope of the x - y plot from the two diagonal voltages U_x and U_y . This slope, $\tan \phi$, is related to the thermal conductivities of the fluids in the measurement and reference cells, λ_y and λ_x , by combining eq 5 and 12 (assuming $k_1 = 0 = k_2$) to give (see Appendix)

$$\begin{aligned} \lambda_y &= \frac{\lambda_x}{\tan \phi} \left[\frac{A_y}{A_x} \right] \left[\left[\frac{R_x^0}{R_y^0} \right]^4 \frac{L_{1x} R_{1y}}{L_{1y} R_{1x}} \right] \\ &= \frac{\lambda_x}{\tan \phi} \left[\frac{A_y}{A_x} \right] C \end{aligned} \quad (15)$$

Determination of the cell constant C as a function of temperature permits determination of the unknown thermal conductivity λ_y relative to that of the reference fluid λ_x using the accurately known resistance quotient A_y/A_x .

Equipment Description

Cell Design. The new cell design employs two mechanically connected platinum wires incorporated into separate arms of a Wheatstone bridge. Variable strain effects, which are difficult to compensate, particularly over large temperature ranges, are effectively eliminated by the subtractive effect. The scant attention devoted to this aspect of cell design is surprising when considering that mechanical strain can produce resistance changes comparable to those of the small induced temperature change. A useful feature of the developed method is that adjustment of the Wheatstone bridge to an equalizing mode will immediately reveal the magnitude of spurious signals such as those arising from thermocouple effects.

The glass, stainless-steel, and Teflon cell shown in Figure 3 is the result of considerable experimentation to eliminate unreproducible strain, thermocouple, and end effects.

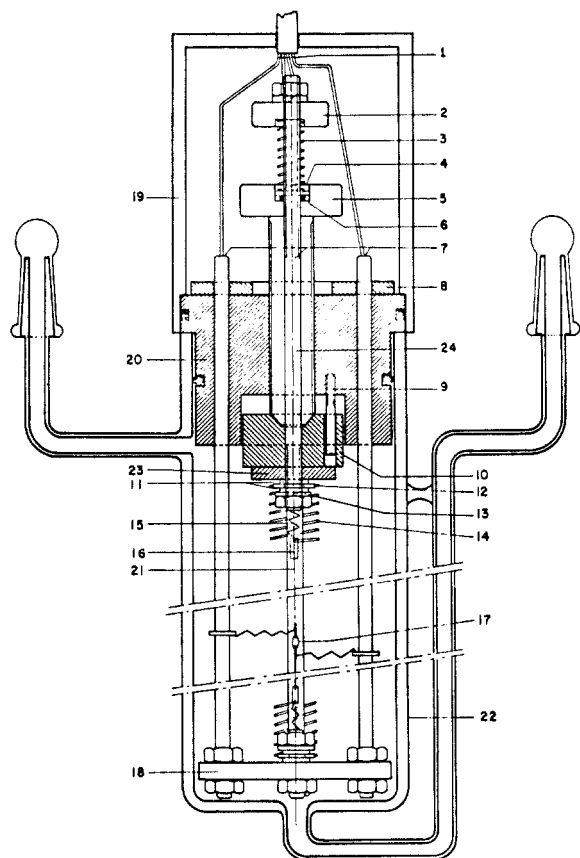
The two-element 20- μm platinum wire (21) is shown suspended between platinum strips (16). The latter are connected through folded 0.0125-mm platinum strips to the stainless-steel rods (24). The wires are lightly tensioned with the stainless-steel spring (14) which is spot welded to the platinum strip (16) but is electrically and thermally insulated from the steel rod with Teflon disks (11).

The construction presents a long thermal conduction path from the heated end of the platinum wire to the stainless steel-platinum junction which is, in effect, a thermocouple. The stainless-steel spring also serves as a heat sink. The construction keeps the steel-platinum junction isothermal during the transient heating process and maintains the long and short wires at the same tension at all temperatures.

From the junction of the long (± 11 cm) and short (± 5 cm) platinum wires (17), connections are made through 0.0125-mm folded platinum strips, which do not alter the wire tension, to the stainless-steel rods (22) of the insert element.

Fine adjustment of the wire tension is made by turning the threaded Teflon bolt (5) while rotation and resulting torque strain on the wire are eliminated by the guide pin (9).

Possible thermocouple effects arising from electrical junctions above the main Teflon plug (20) were avoided or reduced by maintaining an isothermal environment with the perspex covering cap (19). For the y (i.e., nonreference) cell an additional air gap insulated steel cover, heat sunk in the water bath, was



CELL ASSEMBLY: 1) ELECTRICAL LEADS, TWO WIRE SHIELDED CABLE; 2) SPRING HOLDER; 3) SPRING, S.S.; 4) S.S. WASHER; 5) TEFLON BOLT; 6) RUBBER O-RING; 7) S.S. RODS, TYPE 304; 8) COPPER HEATSINK; 9) S.S. GUIDE BOLT; 10) TEFLON CYLINDER; 11) TEFLON WASHERS; 12) S.S. WASHER; 13) S.S. SPRINGWASHER; 14) S.S. SPRING TYPE 304; 15) PLATINUM FOIL; 16) PLATINUM STRIP; 17) ELECTRICAL SEPARATION; 18) TEFLON BOTTOM PART; 19) PERSPEX CAP; 20) TEFLON PLUG; 21) PLATINUM WIRE; 22) GLASS CONTAINER; 23) HEATSINK S.S.; 24) ROD S.S.

Figure 3. Thermal conductivity cell showing insert element and container.

placed over the assembly to cope with larger cell ambient temperature differences.

All internal electrical connections were spot welded, and the platinum wires were annealed at high temperature after assembly by passing a direct current for ~ 30 min. The two cells were made as identical as possible.

Electrical Circuitry. In the twin Wheatstone bridge arrangement shown in Figure 2B, the resistances R_1' , R_2' , R_3 , and R_4 were spool-wound manganin resistors supplied by General Radio with temperature coefficients of < 10 ppm/ $^{\circ}\text{C}$. The bridge components were housed in a metal enclosure, and all external connections were shielded cable.

Multipole gold-plated switches were used to eliminate contact resistances. The sensitivity ranges of the HP7046A x-y recorder were augmented with a precision voltage divider. The galvanometer (G) used for bridge balancing was a Yokogawa log-linear Model 2709 sensitive to 0.20 nA, and the power supply was a Hewlett-Packard Model 6114A precision constant voltage source with load and source effects claimed to be 0.005%. Cell bath temperatures were maintained constant to ± 0.005 $^{\circ}\text{C}$ by using Braun Model 1480 controllers.

Operating Procedure and Reference Standard. The cell constant defined by eq 14 was determined with ethylene glycol (supplied by Merck, density = 1.112–1.113) in both reference and measurement cells with temperatures in the latter varying between -20 and 80 $^{\circ}\text{C}$. Glycol was used as a convenient reference standard since the delayed onset of free convection (due principally to the liquid's high viscosity) produced plots linear over a large range. The reference cell temperature was maintained constant at 25 $^{\circ}\text{C}$.

All thermal conductivity values reported are relative to the reference standard adopted for ethylene glycol, viz.

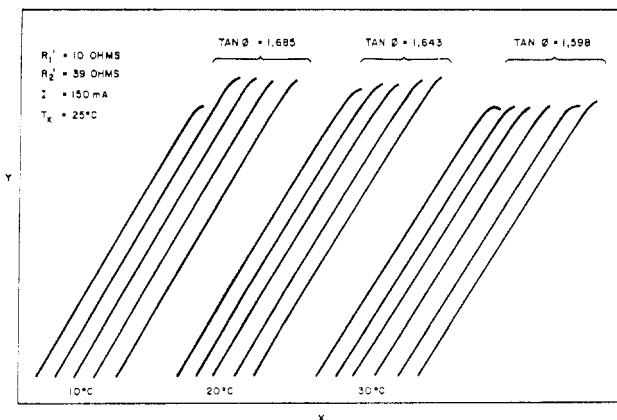


Figure 4. Sample x-y traces for propanol with average slope values indicated.

$$\lambda(\text{W/mK}) = 0.2496 + 0.000209T (T \text{ in } ^{\circ}\text{C})$$

as measured by Grassmann et al. (18). Grassmann's measurements (16) for water at 60.1 $^{\circ}\text{C}$ (0.650 W/mK) based in turn on a standard of 0.596 W/mK for water at 20 $^{\circ}\text{C}$ differs by only 0.58% from the value recommended by McLaughlin (23), and Grassmann's method is considered reliable. If a demonstrably more accurate set of data for ethylene glycol becomes available, the present data should be revised accordingly.

Optimum values of the resistances R_1' and R_2' were found by experimentation (10 and 39 Ω , respectively), their sum being constrained by eq 13. These resistances and a heating current of 150 mA were maintained constant for all experiments. Resistance R_a (1370 Ω) was interposed to produce a bridge balancing current sufficiently small to preclude heating of the cell wires.

Excellent straight-line plots were obtained for 10 alcohols, from methanol to decanol, for the above temperature range. Each thermal conductivity reported is the average of at least four determinations, which could be made at 5–10-min intervals at a given temperature. The chemicals were analytical grade supplied by Merck.

Results and Discussion

The linearity of the plots obtained in all experiments is illustrated by the sample traces for 1-propanol in Figure 4. The absence of initial offset or curvature indicates little influence of finite wire heat capacity. The onset of free convection is reflected by the curvature at the end of the plots.

The experimentally determined cell constant is correlated as a linear function of temperature in Figure 5. At room temperature (25 $^{\circ}\text{C}$) the measured cell constant is in exact agreement with that predicted by eq 15. At other temperatures some residual extraneous effect identifiable with the last terms in eq 11a and 11b appears operative.

Typical precision and linearity of thermal conductivity with temperature are shown for 1-octanol in Figure 6. Thermal conductivity at 0 $^{\circ}\text{C}$, temperature coefficient, claimed purity, and a refractive index comparison with literature data (24) are shown for the 10 alcohols in Table I, and measured data at various temperatures are summarized in Table II. The precision of the data is estimated to be 0.5% except for methanol where, because of the rapid onset of free convection, the precision decreases to $\pm 1\%$.

In Figures 7–16 thermal conductivities measured for the 10 alcohols as functions of temperature are compared with literature data from ref 25 unless otherwise indicated. The most striking feature of these presentations is the extent of the discrepancies, particularly in temperature coefficient, in the results of different investigators. For 1-heptanol, for example, discrepancies in thermal conductivity exceeding 15% and in temperature coefficient exceeding 250% are evident.

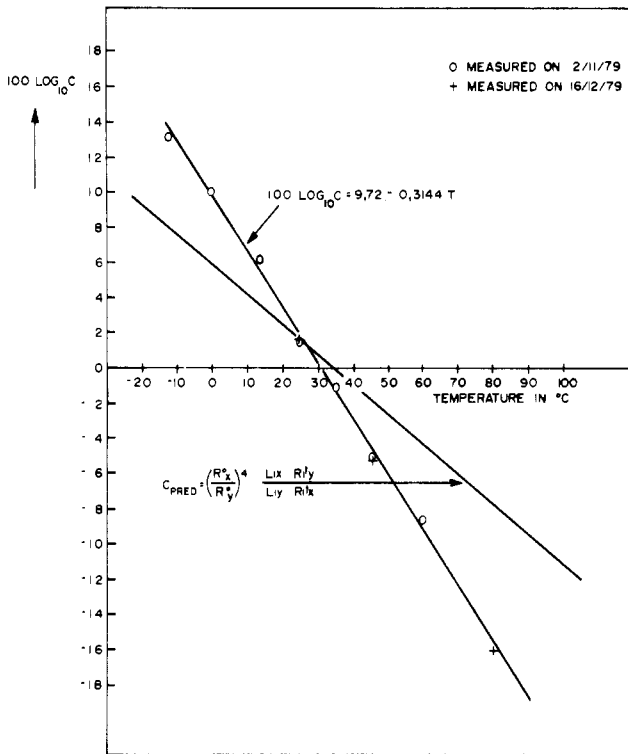


Figure 5. Logarithm of cell constant as a function of temperature.

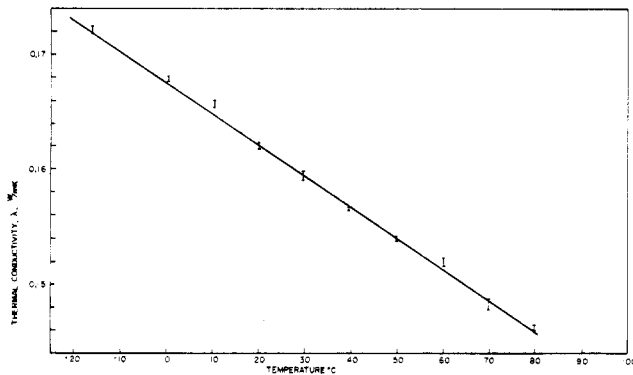


Figure 6. Thermal conductivity of octanol as a function of temperature.

Table I. Alcohol Property Data

alcohol	claimed purity, wt %	refractive index (n_{20}^D)		thermal conductivity (λ) at 0 °C, W/mK	temp coeff ($d\lambda/dT$), mW/mK ²
		measd	lit. ^a		
methanol	99.5	1.3280	1.3288	0.206	-0.26
ethanol	99.8	1.3609	1.3611	0.1779	-0.251
1-propanol	99.0	1.3844	1.3850	0.1628	-0.234
1-butanol	99.5	1.3987	1.3993	0.1590	-0.208
1-pentanol	98.5	1.4090	1.4101	0.1579	-0.177
1-hexanol	98.0	1.4172	1.4178	0.1601	-0.176
1-heptanol	98.0	1.4231	1.4249	0.1656	-0.247
1-octanol	97.0	1.4285	1.4295	0.1674	-0.270
1-nonanol	96.0	1.4336	1.4333	0.1726	-0.260
1-decanol	97.0	1.4366	1.4372	0.1665	-0.232

^a Reference 24.

In general the data in best agreement with those of the present study are those of Tufeu (26), Vargaftik (27), and Abas-Zade (28). Except in the case of methanol, the data measured by Jamieson et al. (25) are consistently lower than those of the present study. For methanol the recent data of Takizawa et al. (29) are in good agreement with present results.

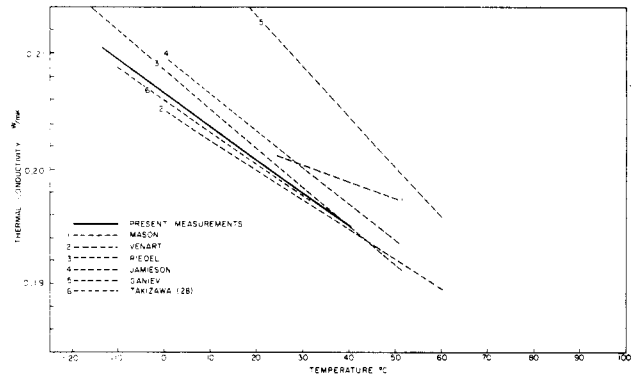


Figure 7. Thermal conductivity of methanol.

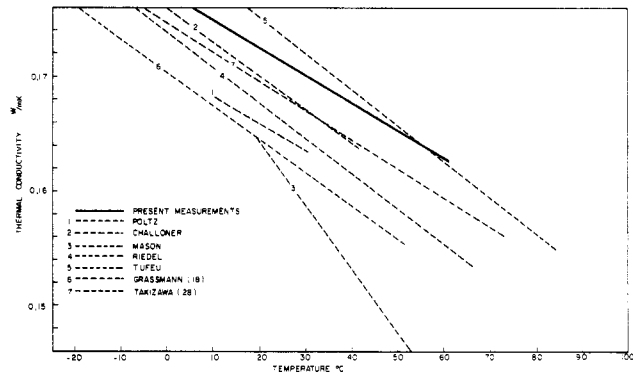


Figure 8. Thermal conductivity of ethanol.

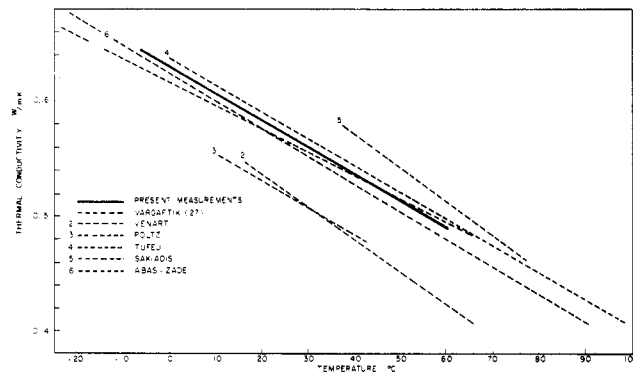


Figure 9. Thermal conductivity of 1-propanol.

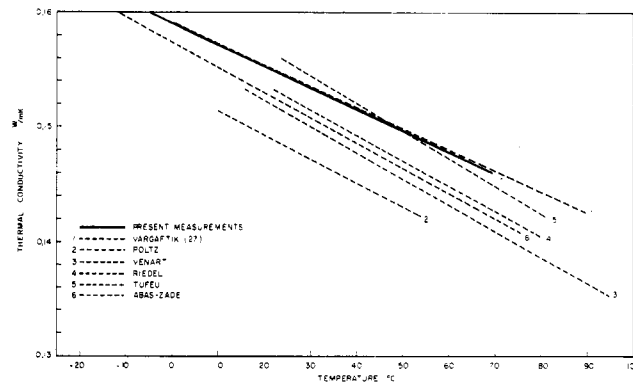


Figure 10. Thermal conductivity of butanol.

Evaluation of the accuracy of published liquid thermal conductivity data is a difficult task. An absolute test, such as evaluation of the Eucken factor for noble gases, is not available for liquid data, and essentially heuristic criteria involve judgment of equipment design, accuracy of signal measurement, and error compensation. The temperature coefficient of thermal

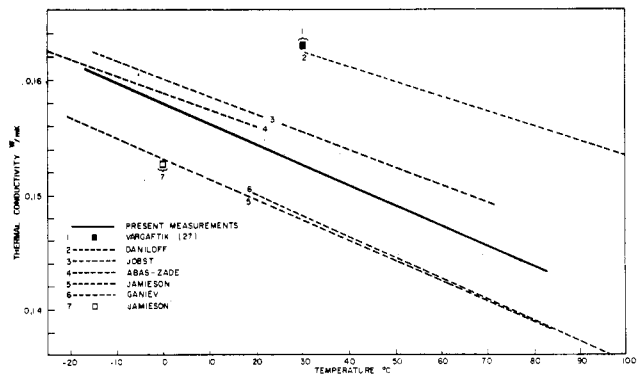


Figure 11. Thermal conductivity of 1-pentanol.

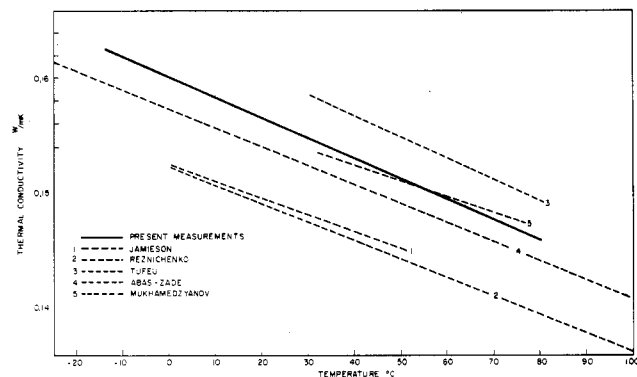


Figure 12. Thermal conductivity of 1-hexanol.

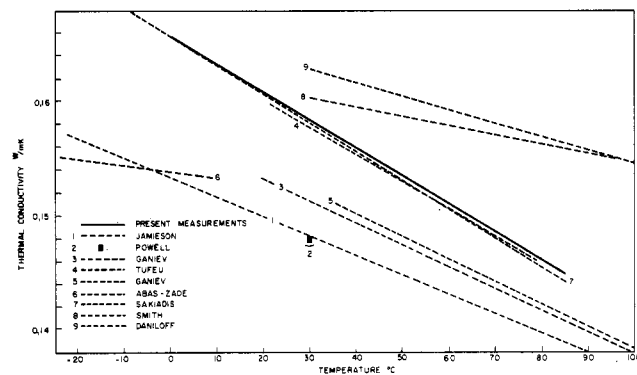


Figure 13. Thermal conductivity of 1-heptanol.

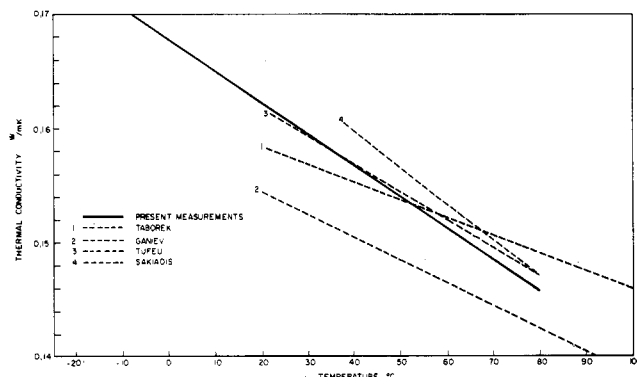


Figure 14. Thermal conductivity of 1-octanol.

conductivity is particularly sensitive to small systematic errors which may arise from thermocouple, strain, radiative, or end effects when measuring over large temperature ranges.

Advances in the theory of the molecular energy transport in liquids which could produce a stringent practical criterion for judging temperature coefficients of thermal conductivity, even

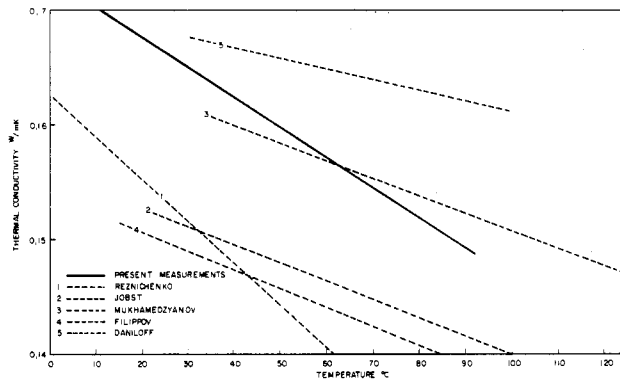


Figure 15. Thermal conductivity of 1-nonanol.

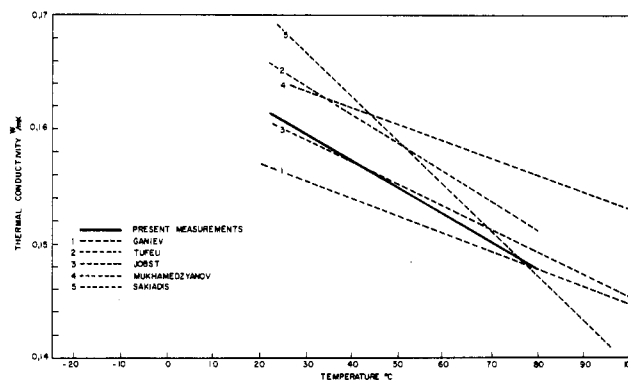


Figure 16. Thermal conductivity of 1-decanol.

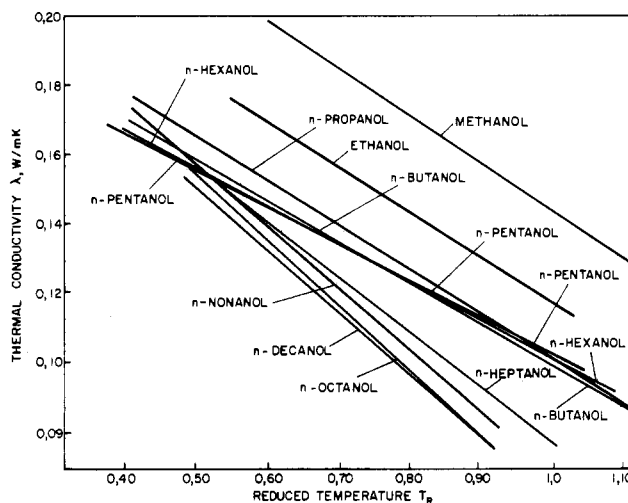


Figure 17. Thermal conductivity vs. reduced temperature.

for a limited class of compounds, would prove invaluable in further equipment development.

For members of a homologous series (as in the present study), an interpretation of the corresponding states theory by Saklades and Coates (30) suggests that at the critical temperature thermal conductivities extrapolated from low-temperature data will converge to a point for all members and that temperature coefficients should vary regularly from member to member. In Figures 17 and 18 these predictions are tested.

In Figure 17 the expectation (30) that at the same reduced temperature the thermal conductivity for all members of a series should decrease with molecular mass is obeyed only approximately. Also, the lines, extrapolated from thermal conductivity at low temperatures, fail to converge to a single point near the critical temperature as found by Saklades and Coates (30) for aliphatic hydrocarbons. Convergence of the lines near

Table II. Measured Thermal Conductivities (λ , W/mK) for Normal Alcohols^a

temp, °C	methanol		ethanol		propanol		butanol		pentanol		hexanol		heptanol		octanol		nonanol		decanol					
	S	λ	S	λ	S	λ	S	λ	S	λ	S	λ	S	λ	S	λ	S	λ	S	λ				
-16.75											0.6	0.1624												
-15.9															0.7	0.1724								
-14.0	2	0.209																						
-13.5								0.5	0.164															
-11.2							0.5	0.166																
-5.0				0.179																				
-3.7											0.6	0.1608												
0.0	1	0.207				0.8	0.162	0.2	0.1585	0.6	0.1587					0.4	0.1681							
10.0	0.3	0.204				0.6	0.1603	0.2	0.1568	0.5	0.1558	1	0.1580	0.3	0.1629	0.4	0.1657							
13.0																								
15.0				0.58	0.174															0.40	0.1687			
20.0	2	0.203				0.60	0.1585	0.2	0.1564	0.5	0.1542	0.4	0.1572	0.8	0.1602	0.6	0.1620							
25.0				0.96	0.1714															0.43	0.1662			
30.0	2	0.198				0.5	0.155	1	0.1525	0.5	0.1518	0.6	0.1540	0.5	0.1583	0.9	0.1591				0.3	0.1596		
35.0				0.42	0.169															0.64	0.1636			
40.0	4	0.195				0.6	0.1544	0.5	0.1503	0.3	0.1511	0.5	0.1537	0.8	0.1566	0.3	0.1564				0.2	0.1595		
45.0				0.41	0.1663															1.50	0.1609			
50.0						0.5	0.1508	0.4	0.1492	0.3	0.1494	0.7	0.1523	0.6	0.1536	0.3	0.1540					0.2	0.1554	
55.0				0.56	0.1645																0.94	0.1583		
60.0						0.5	0.1485	0.4	0.1473	0.4	0.1470	0.6	0.1491	0.4	0.1512	0.7	0.1518				0.19	0.1558		
65.0																								
70.0								0.5	0.1460	0.6	0.1461	0.3	0.1461	0.3	0.1480	1	0.148					0.5	0.1504	
80.0										0.9	0.1437	0.8	0.1452	0.4	0.1454	0.5	0.1460						0.5	0.1482

^a S = measurement standard deviation $\times 10^3$.

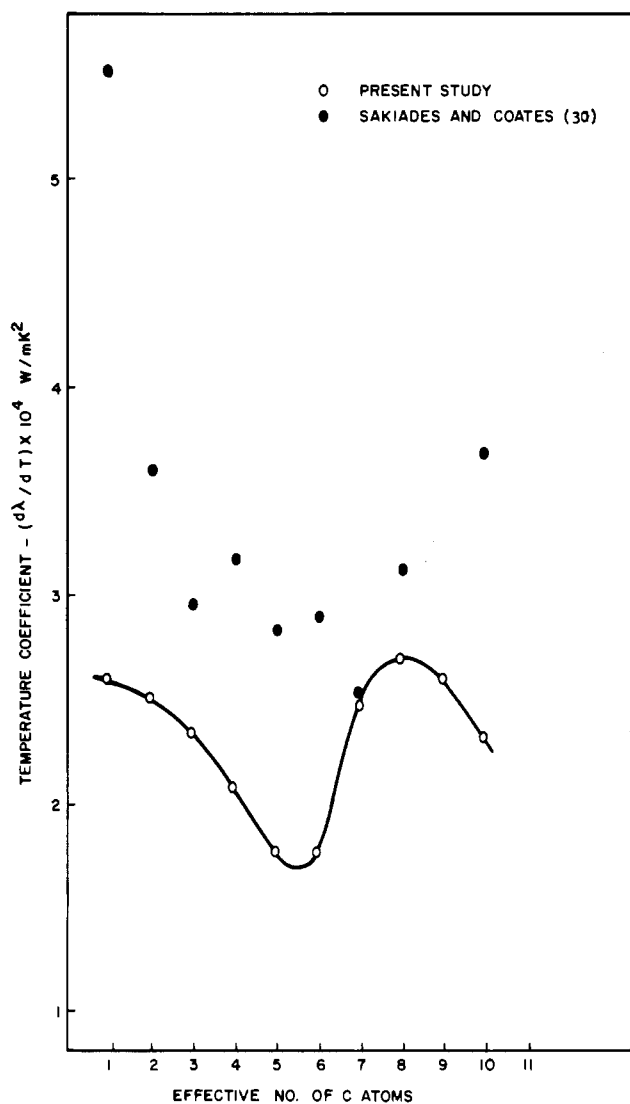


Figure 18. Temperature coefficient of thermal conductivity vs. effective number of carbon atoms.

$Tr = 1.0$ is found only approximately for intermediate members of the series from propanol to hexanol, suggesting that the corresponding states theory requirement (30) that the (non-spherical) molecules should have the same shape factor is valid only for these intermediate members. The results are contrary to those obtainable from the data of Sakiades and Coates (30) (not shown) for which convergence near $Tr = 1.0$ is found only for the first three members of the alcohol series.

The temperature-coefficient data (Figure 18) contrast with those of Sakiades and Coates (30), who expected and claimed a "regular" variation from member to member not apparent in their data. The temperature coefficient for methanol (-0.26 mW/mK²) is in good agreement with the average (-0.25) for data rated accurate to within 2% by Jamieson and Irving (25) and suggests that the very high value (-0.55) measured by Sakiades and Coates is incorrect. Their value for 1-decanol (-0.367 mW/mK²), similarly, is much higher than that of the present study (-0.232) or of the average (-0.186 mW/K²) reported in the literature (25).

The very smooth, apparently periodic variation of temperature coefficient with number of carbon atoms in Figure 18 has not previously been found by other workers and could easily be obscured in previous work by temperature-dependent errors. Interpretation of the effect shown presents an interesting challenge, and we recommend that, in further studies of thermal conductivity of homologous series, the temperature coefficients should be examined for similar regular variations.

Conclusion

The two-wire thermal conductivity cell, with heater elements mechanically coupled to ensure uniform strain at all temperatures, performed well and closely approximates a uniform line source in an infinite fluid. The excellent linear response obtained in all experiments with twin cells used in a relative configuration supports our conviction that the main sources of error have been eliminated. The method is rapid, and the onset of free convection or any equipment fault is readily detected.

In absolute transient methods where constancy of heating rate has not been ensured (as in the present study), the slope of a ΔT vs. $\ln t$ plot should be corrected by using eq 10 or Figure 1.

The thermal conductivities and temperature coefficients obtained for 10 aliphatic alcohols from methanol to decanol are considered to be reliable. The smooth periodic variation of temperature coefficient with number of carbon atoms for the series has not previously been found and merits study. We hope that the method and the data presented will be useful in further refinement of equipment and of theoretical prediction which, presently, is either too complex for engineering application or of limited applicability because of empirical assumptions.

Acknowledgment

We are indebted to F. Birnie for assistance in the experimental work.

Appendix

Derivation of Eq 12. Assume that resistances of long and short heated elements in Figure 2B are given by

$$R_1^t = R_1^0(1 + \alpha\Delta T) + k_1\Delta T \quad (A1)$$

$$R_2^t = R_2^0(1 + \alpha\Delta T) + k_2\Delta T \quad (A2)$$

where k_1 and k_2 are thermocouple or strain coefficients. The diagonal voltage U_y arising at time t after passage of a heating current I^t through the resistances R_1 and R_2 for an applied voltage U is

$$U_y = I^t(R_1^t + R_2^t) - I^0(R_1^0 + R_2^0) \\ = \frac{U(R_1^t + R_2^t)}{R_1^t + R_2^t + R_1^0 + R_2^0} - \frac{U(R_1^0 + R_2^0)}{R_1^0 + R_2^0 + R_1^0 + R_2^0}$$

(assuming a large impedance instrument connection across U_y). Denoting denominators in the above equation by R^t and R^0 , respectively

$$U_y/U = \frac{R^0(R_1^t + R_2^t) - R^t(R_1^0 + R_2^0)}{R^0 R^t}$$

Substitution of eq A1 and A2 into the above equation yields, after simplification

$$U_y/U = \frac{\alpha\Delta T(R_1^0 R_2^t - R_2^0 R_1^t) + (k_1 - zk_2)(R_2^0 + R_2^t)\Delta T}{R^0 R^t} \quad (A3)$$

Equation A3 (=eq 12) is rigorous for resistances behaving according to eq A1 and A2 and can be used to obtain thermal conductivities by the absolute method (which requires a ΔT -ln (time) data set) if $k_1 - zk_2$ is known. In the usual case where $k_1 - zk_2$ is not known, experimental U_y -time values obtained from a single cell can be converted to a ΔT -ln (time) data set using a trial and error procedure which will be described in a later publication.

Derivation of Eq 15 (Measured Slope- λ Relationship). In the case $k_1 - zk_2 = 0$ (i.e., no extraneous thermocouple or strain effects), the temperature rise in the y cell is, from eq A3

$$\Delta T_y = \frac{(R^0 R^t)_y}{\alpha A_y} \frac{U_y}{U}$$

A similar equation with different subscripts holds for cell x. Thus for heating elements of the same material in x and y cells

$$\frac{(\Delta T)_y}{(\Delta T)_x} = \frac{(R^0 R^t)_y}{(R^0 R^t)_x} \frac{A_x}{A_y} \frac{U_y}{U_x} \quad (A4)$$

Noting that $U_y/U_x =$ measured slope $= \tan \phi$ and that

$$\frac{(\Delta T)_y}{(\Delta T)_x} = \left[\frac{q_y}{q_x} \right] \left[\frac{\lambda_x}{\lambda_y} \right]$$

for two ideal line sources heated simultaneously, eq A4 becomes

$$\lambda_y = \frac{\lambda_x}{\tan \phi} \frac{q_y (R^0 R^t)_x A_y}{q_x (R^0 R^t)_y A_x}$$

The heating rate per unit length q is the same for both elements of a cell, e.g.

$$q_y = I^2 R_{1y}^t / L_{1y} = I^2 R_{2y}^t / L_{2y} \\ \doteq \frac{U^2 R_{1y}^0}{(R_y^0)^2 L_{1y}} \quad \text{if } R_1^0 + R_2^0 = R_1^t + R_2^t \quad (\eta = 0)$$

$$\therefore \lambda_y = \frac{\lambda_x}{\tan \phi} \frac{A_y}{A_x} \left[\left(\frac{R_x^0}{R_y^0} \right)^4 \frac{L_{1x} R_{1y}}{L_{1y} R_{1x}} \right] \quad (A5)$$

$R_x^t/R_y^t = R_x^0/R_y^0$, a good approximation for small temperature rise. The term in square brackets in eq A5 is the cell constant of eq 15.

Glossary

A	resistance coefficient defined in eq 14, Ω^2
a	wire diameter, m
b	cell diameter, m
C	cell constant
F	correction factor defined in eq 6, dimensionless
I	current, A
K	temperature rise-ln (time) correction factor, dimensionless
k	strain-end effect coefficient, Ω/K
L	length of heated wire
q	heat generation per unit length, W/m
R	resistance, Ω
r	radial coordinate, m
T	temperature
ΔT	temperature rise
\bar{T}	dimensionless temperature defined in eq 9
U	voltage
z	$(R_1^0 + R_1^t)/(R_2^0 + R_2^t)$

Greek Letters

α	resistance temperature coefficient, $^{\circ}\text{C}^{-1}$
η	resistance difference ratio, dimensionless
λ	thermal conductivity, W/mK
$\tan \phi$	slope of linear portion of plotter trace, dimensionless

Subscripts

R	reduced
x	reference cell or bridge
y	nonreference cell or bridge
1	long heated wire
2	short heated wire

Superscripts

0	value at start of heating period
t	value at time t after start of heating period

Literature Cited

- Poltz, H.; Jugel, R. *Int. J. Heat Mass Transfer* 1967, 10, 1075.
- Stålmane, B.; Pyk, S. *Tek. Tidskr.* 1931, 61, 389.
- Van der Held, E. F. M.; Van Druenen, F. G. *Physica* 1949, 15, 865.
- Van der Held, E. F. M. *Appl. Sci. Res.* 1952, 3, 237.
- Van der Held, E. F. M.; Hardelbol, J.; Kalshoven, J. *Physica* 1953, 19, 208.
- Gillam, D. G.; Romben, L.; Nissen, H.; Lamm, O. *Acta Chem. Scand.* 1955, 9, 641, 657.

- (7) Jamieson, D. T.; Irving, J. B. "Advances in Thermal Conductivity"; Reischig, R., Sauer, J., Eds.; University of Missouri—Rolla: Rolla, MO, 1974; p 185.
- (8) Horrocks, J. K.; McLaughlin, E. *Proc. R. Soc. London, Ser. A* **1963**, *273*, 259.
- (9) De Castro, C. A.; Calado, J. C. G.; Wakeham, W. A. *J. Phys. E* **1976**, *9*, 1073.
- (10) Weishaupt, J. *Forschung* **1940**, *11*, 20.
- (11) De Groot, J. J.; Kestin, J.; Sooklazzan, H. *Physica* **1974**, *75*, 454.
- (12) Haarman, J. W. *Physica* **1971**, *52*, 605.
- (13) Haarman, J. W.; Thesis, Technische Hogeschool, Delft, Holland, 1969.
- (14) Kestin, J.; Ro, S. T.; Wakeham, W. A. *Physica* **1972**, *58*, 165.
- (15) De Castro, C. A.; Wakeham, W. A. *Therm. Conduct.* **1978**, *15*.
- (16) Grassmann, P. Doctoral thesis, no. 3078, Federal Institute of Technology, Zürich, Switzerland, 1960.
- (17) Grassmann, P.; Straumann, W. *Int. J. Heat Mass Transfer* **1960**, *1*, 50.
- (18) Grassmann, P.; Straumann, W.; Wildmer, F.; Jobst, W. *Prog. Int. Res. Thermodyn. Transp. Prop., Pap. Symp. Thermophys. Prop., 2nd*, **1962**, *1962*, 447.
- (19) Carslaw, H. A.; Jaeger, J. C. "Conduction of Heat in Solids", 2nd ed.; Oxford University Press: London, 1959.
- (20) Healy, J. J.; de Groot, J. J.; Kestin, J. *Physica B & C (Amsterdam)* **1976**, *82*, 392.
- (21) Shampine, L. F.; Allen, R. C. "Numerical Computing"; W. B. Saunders: Philadelphia, PA, 1973.
- (22) Davis, P. J.; Rabinowitz, P. "Numerical Integration"; Blaisdell Publishing Co.: Waltham, MA, 1967.
- (23) McLaughlin, E. *Chem. Rev.* **1964**, *64*, 389.
- (24) Weast, R. C., Ed. "Handbook of Chemistry and Physics", 56th ed.; CRC Press: Cleveland, OH, 1974.
- (25) Jamieson, D. T.; Irving, J. B.; Tudhope, J. S. "Liquid Thermal Conductivity—A Data Survey to 1973"; HM Stationery Office: Edinburgh, United Kingdom, 1975.
- (26) Tufeu, R., et al., as given in ref 25.
- (27) Vargaftik, N. B. "Tables on the Thermophysical Properties of Liquids and Gases", 2nd ed.; Hemisphere: Washington, DC, 1975 (also as given in ref 25).
- (28) Abas-Zade, A. K., as given in ref 25.
- (29) Takizawa, S.; Murata, H.; Nagashima, A. *Bull. JSME* **1978**, *21*, 273.
- (30) Saklades, B. C.; Coates, J. *AIChE J.* **1955**, *1*, 275.

Received for review August 11, 1980. Accepted April 14, 1981.

Enthalpies of Vaporization and Vapor Pressures of Triphenyl-, Tri(*p*-tolyl)-, and Tris(2-cyanoethyl)phosphines

Kees G. de Krulf*

Chemical Thermodynamics Group, State University of Utrecht, Utrecht, The Netherlands

Johan M. Herman and Pieter J. van den Berg

Department of Chemical Technology, Delft University of Technology, 2628 BL Delft, The Netherlands

Simultaneous torsion and mass loss effusion techniques were used to measure the vapor pressure as a function of temperature. The enthalpies of sublimation/vaporization were derived from the temperature dependence of vapor pressure. Overall mean values for both techniques are as follows: triphenylphosphine (liquid), $\Delta H_v^\circ(378.06 \text{ K}) = 91.4 \pm 2 \text{ kJ mol}^{-1}$, $p(378.06 \text{ K}) = 4.0 \pm 0.1 \text{ Pa}$; tri(*p*-tolyl)phosphine (liquid), $\Delta H_v^\circ(385.28 \text{ K}) = 126 \pm 5 \text{ kJ mol}^{-1}$, $p(385.28 \text{ K}) = 0.40 \pm 0.01 \text{ Pa}$; tris(2-cyanoethyl)phosphine (solid), $\Delta H_v^\circ(412.60 \text{ K}) = 105.7 \pm 2 \text{ kJ mol}^{-1}$, $p(412.60 \text{ K}) = 0.40 \pm 0.01 \text{ Pa}$.

Introduction

Lately hydridocarbonyltris(triphenylphosphine)rhodium(I), dissolved in triphenylphosphine (TPP) and capillary condensed into the pores of a support, has been successfully applied as a heterogenous catalyst in the industrially important hydroformylation of propylene, i.e., the conversion of propylene, hydrogen, and carbon monoxide to *n*- and isobutyraldehyde (1, 2). In order to calculate the maximum vaporization losses of TPP in a large-scale chemical reactor under reaction conditions, one must know its vapor pressure as a function of temperature. Since only few data could be found in the literature (3), it was decided to measure them. Because tri(*p*-tolyl)phosphine (TTP) and tris(2-cyanoethyl)phosphine (TCP) are also suitable solvents for hydridocarbonyltris(triphenylphosphine)rhodium(I), the vapor pressures of these materials were also measured. In this paper the results of this study are presented.

Experimental Section

Samples. TPP was obtained from Fluka (Switzerland). As preliminary measurements gave spurious results, we further purified TPP by zone refining.

TTP obtained from K & K laboratories Inc. appeared to contain brown impurities which were the cause of low vapor pressures and inconsistent enthalpies of sublimation. Also a sample kindly provided by the Van't Hoff Laboratory (University of Amsterdam) was insufficiently pure. Vacuum sublimation of this sample (400 \rightarrow 300 K at 10^{-5} torr) improved results considerably (1 torr = 101325/760 Pa).

TCP was provided by Strem (USA) and could be used without additional purification.

Measuring Principle. Use was made of the simultaneous torsion and mass loss effusion technique. The apparatus described previously (4) is checked frequently on naphthalene of which very accurate vapor pressure data are given by Ambrose (6).

Treatment of Results. Vapor pressures obtained from simultaneous torsion effusion measurements (subscript t) and mass loss effusion measurements (subscript m) were fitted independently to the equation (5)

$$R \ln (p/p^\circ) = -\Delta G^\circ(\theta)/\theta + \Delta H^\circ(\theta)(1/\theta - 1/T) \quad (1)$$

in which θ is a reference temperature and p° a standard pressure (taken to be 1 Pa). In our measurements over a temperature range of 20 K, the plot of $\ln (p/p^\circ)$ as a function of $1/T$ does not deviate significantly from a straight line. therefore, our results can be described adequately by two parameters, namely, $\Delta G^\circ(\theta)$ and $\Delta H^\circ(\theta)$.